Published in the Russian Federation
International Journal of Environmental Problems
Has been issued since 2015.
ISSN: 2410-9339
E-ISSN: 2413-7561
Vol. 3, Is. 1, pp. 4-13, 2016

DOI: 10.13187/ijep.2016.3.4
www.ejournal33.com

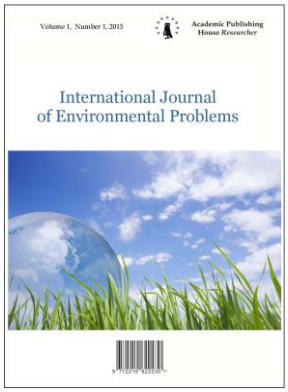

Relevant Topic

UDC 63.54

Application of Remote Sensing for Monitoring of Subsurface Coal Fire: a Case Study in Khanh Hoa Coal Mine, Thai Nguyen Province, Vietnam

Le Hung Trinh

Le Quy Don Technical University, 236 Hoang Quoc Viet, Hanoi, Vietnam
Email: trinhlehung125@gmail.com

Abstract

The Khanh Hoa coal mine is a surface coal mine in the Thai Nguyen province, which is one of the largest deposits of coal in the Vietnam. In recent years due to many reasons such as backward mining techniques and unauthorized mining caused subsurface coal fire in this area. Coal fire is a dangerous phenomenon which seriously affects the environment by releasing toxic fumes, causes forest fires and subsidence of infrastructure surface. This article presents study on the application of LANDSAT multi – temporal thermal infrared images, which help to detect coal fire. The results obtained in this study can be used to monitor fire zones so as to give warnings and solutions to prevent coal fire.

Keywords: subsurface fire, remote sensing, thermal infrared, LANDSAT, land surface temperature.

1. Introduction

Located in Southeast Asia, Vietnam is rich in mineral resources - precious potential resource for the country. Vietnam has big reserves of fossil energy with 10 billion tons of anthracite coal, more than 200 billion tons of brown coal in the northern delta area [1]. As most coal producing countries, Vietnam also has a serious coal fire problem, like USA, South Africa, Venezuela, China and India [6]. Coal fire is caused by the spontaneous combustion of coal during coal oxidation. A very recent, coal fire has been reported in the Nong Son coal mine (Quang Nam province, in 2014), Ha Lam, Thong Nhat, Khe Chuoi, Hong Thai coal mines (Quang Ninh province, in 2004, 2011) and Khanh Hoa coal mine (Thai Nguyen province, in 2014).

To control and mitigate coal fires, researchers in various countries have investigated coal combustion. Remote sensing with many advantages over traditional method has been effectively used for detecting and monitoring coal fire. In 1963, many researches in United States have used thermal remote sensing (TIR) techniques to monitor coal fire and its propagation. Since then, TIR has proven to be a reliable and useful tool for identifying subsurface coal fires. Cracknell, Mansor (1992), Prakash et at. (1999) used the Landsat 5 TM thermal infrared band to identify surface and subsurface fires in Jharia coalfields (India) and calculate the area of surface fires [2, 4]. Voigt et al (2004) described and integrated satellite image approach for detection and monitoring of near surface coal seam fires by observing subtle land surface changes induced by the fires [11]. Prasun et

al (2005) used Landsat 5 TM thermal band data for calculating surface temperature along with NDVI to identify coal fire in the Raniganj coalbelt, India [5]. Mishra et al (2014) found a correlation between satellite image temperature and surface temperature of the Jharia coalfield [6]. Mishra et al. (2012) estimated of air pollution concentration over Jharia coalfield and established a relation between satellite imagery and ground data. Based on this study, Mishra et al. proved that, the eastern part of Jharia coalfield was more polluted in comparison to the western part due to extensive mining activities as well as a large number of coal fires [7]. Chen et al (2007) based a combination of multi-temporal thermal infrared data, high spatial resolution remote sensing data and field measurements to detect coal fires dynamics in the Inner Mongolia Autonomous region in northern China [3]. Huo et al. (2014) used multi-temporal nighttime Landsat SWIR and TIR data to identify the thermal anomalies related to subsurface coal fires on the Rujigou coalfield (Northwest China) [8]. Gautam et al. (2008) used NOAA/AVHRR data to detect the surface hot spot of Jharia coalfield region by developing an algorithm to find out the subsurface hot spot with operational satellite data [9].

This paper focused on detection and dynamics of coal fire in Khanh Hoa coal mine, Thai Nguyen province (Vietnam) using Landsat multi-temporal thermal infrared data.

2. Study area and materials

Study area. The Khanh Hoa coal mine (Fig. 1) is located in the northern of Thai Nguyen city, about 80 km northeast of Hà Noi, the capital of Vietnam. The area is bounded by 21°36'7"N latitude and 105°46'59"E longitude. Coal mining is an important contributor to the development of local social economy, but also has negative impact on the environment, such as water and air pollution, coal fire. In the recent years, the Khanh Hoa coal mine has been affected by many coal fires [15].

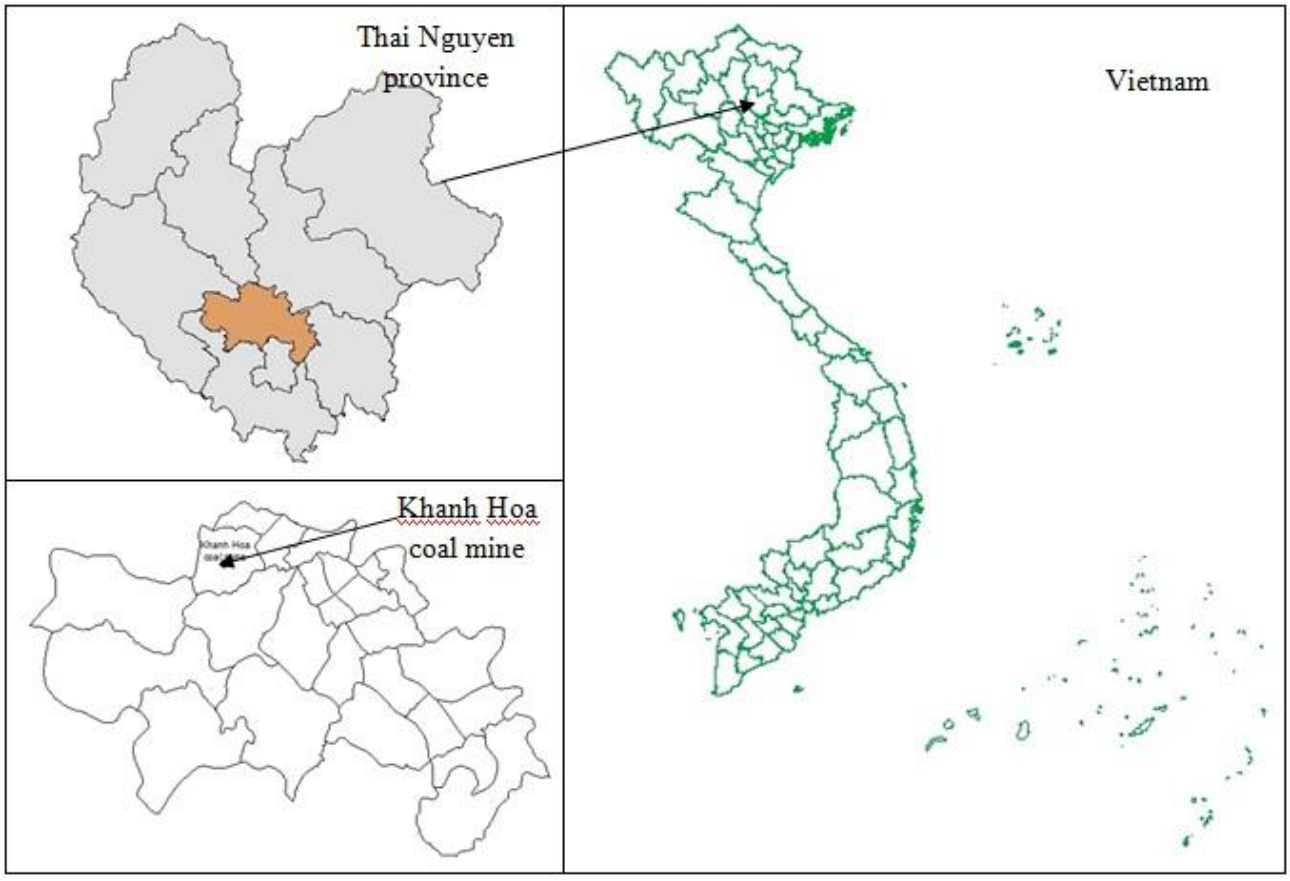

Figure 1. The study area, Khanh Hoa coal mine, Thai Nguyen province (Vietnam)

Data used. In this study, multi-temporal cloud – free Landsat 5 TM, Landsat 7 ETM+ and Landsat 8 OLI data were collected (Figure 2a, 2b, 2c). All the Landsat data were the standard terrain correction products (L1T), downloaded from United States Geological Survey (USGS – http://glovis.usgs.gov) website. The data used in this study was grouped into two categories (Table 1): the thermal infrared data was used to calculate temperature, the red and near infrared band to calculate surface emissivity based on normalized difference vegetation index (NDVI).

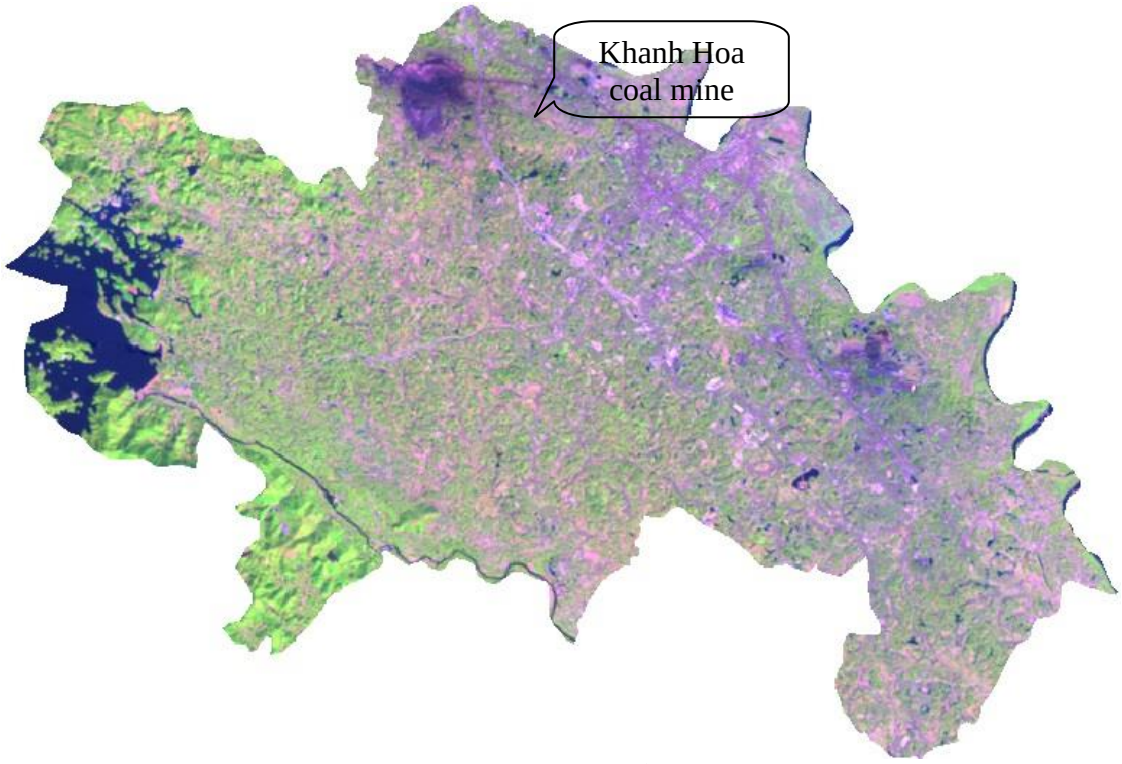

a)

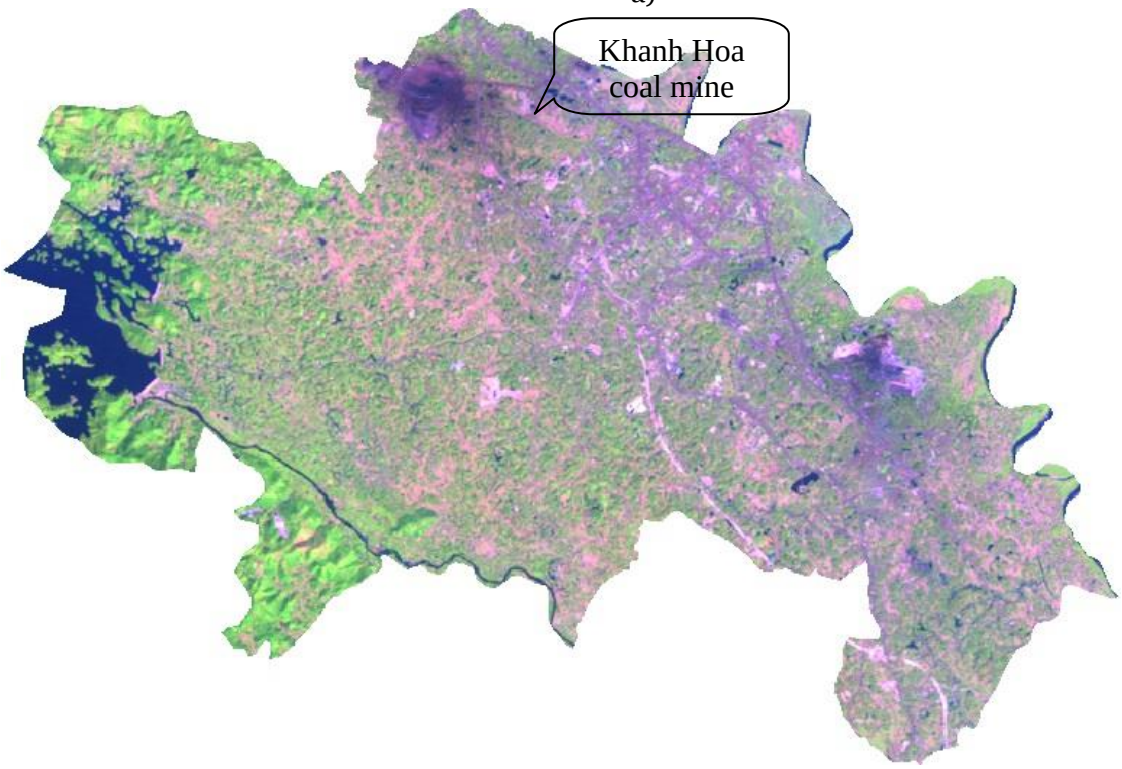

b)

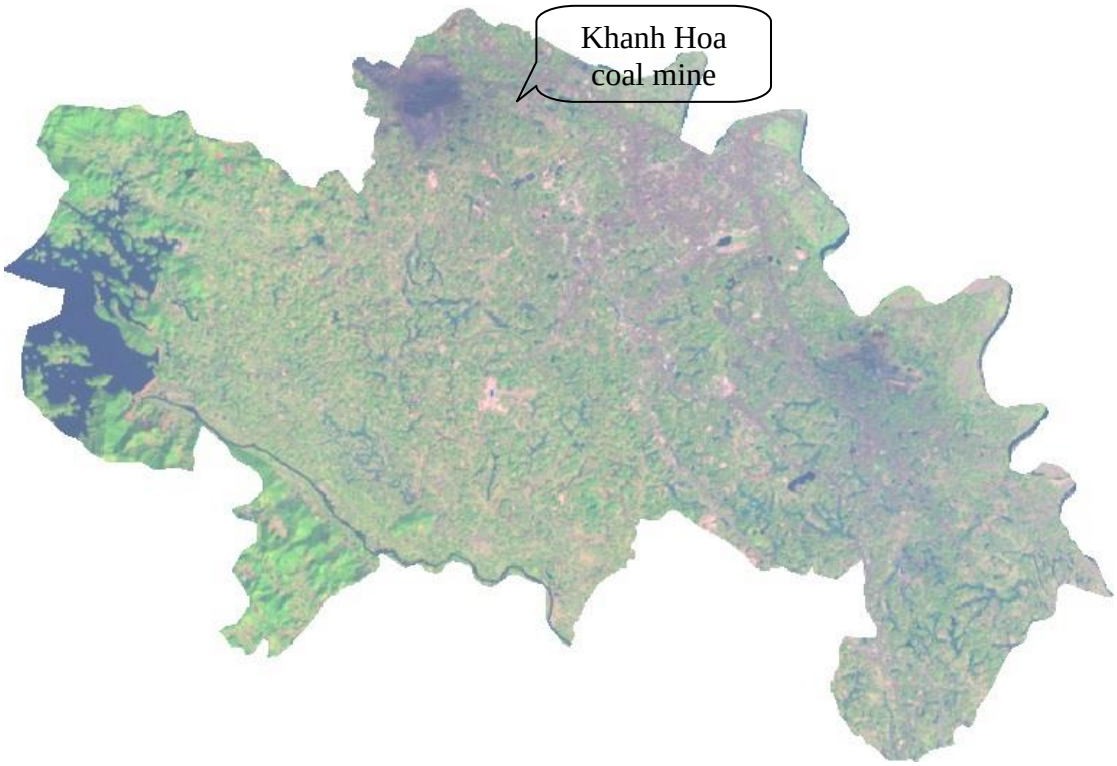

c)

Figure 2. Landsat multispectral image of the Thai Nguyen city 08 November 2007 (a), 08 November 2010 (b) and 19 January 2014 (c)

Table 1. The Landsat data used for NDVI and temperature retrieval to coal fire detection in the study

No.	Data type	Band used for temperature	Band used for NDVI	Time of data acquisition
1	Landsat 7 ETM+	6	3, 4	8 November 2007
2	Landsat 5 TM	6	3, 4	8 November 2010
3	Landsat 8 OLI	10	4, 5	19 January 2014

3. Methodology

3.1. Conversion of the digital number to spectral radiance

Image processing started with radiometric and geometric correction. Radiometric correction done by converted the digital number value to radiance value. Based on NASA model, the digital values of thermal band Landsat 5 TM and Landsat 7 ETM+ were converted to spectral radiance ($Wm^{-2}\mu m^{-1}$) using following equation [14]:

$$L_\lambda = \frac{Lmax_\lambda - Lmin_\lambda}{Q_{calmax} - Q_{calmin}} (Q_{cal} - Q_{calmin}) + Lmin \qquad (1)$$

Where

L_λ - Spectral radiance at the sensor's aperture [W/(m².sr.μm)]

Q_{cal} – Quantized calibrated pixel value

Q_{calmax} – Maximum quantized calibrated pixel value corresponding to $Lmax_\lambda$

Q_{calmin} – Minimum quantized calibrated pixel value corresponding to $Lmin_\lambda$

$Lmax_\lambda$ - Spectral at sensor radiance that is scaled to DNmax [W/(m².sr.μm)]

$Lmin_\lambda$- Spectral at-sensor radiance that is scaled to DNmin [W/(m².sr.μm)]

Table 2. Landsat TM and ETM+ spectral radiance $Lmax_\lambda$, $Lmin_\lambda$ dynamic ranges [14]

No.	Data type	Band	$Lmax_\lambda$	$Lmin_\lambda$
1	Landsat 7 ETM+	6.1 Low gain	17.04	0.0
		6.2 High gain	12.65	3.2
2	Landsat 5	6	15.3032	1.2378

Landsat 8 OLI and TIRS band data can be converted to spectral radiance using the radiance rescaling factors provided in the metadata file [14]:

$$L_\lambda = M_L.Q_{cal} + A_L \quad (2)$$

Where

M_L - Band specific multiplicative rescaling factor from the metadata (RADIANCE_MIUL_BAND_x, where x is the band number)

A_L - Band specific additive rescaling factor from the metadata (RADIANCE_ADD_BAND_x, where x is the band number)

Q_{cal} - Quantized and calibrated standard product pixel values (DN)

Table 3. Landsat 8 TIRS spectral radiance M_L, A_L dynamic ranges [14]

No.	Data type	Band	M_L	A_L
1	Landsat 8 TIRS	10	$3.3420.10^{-4}$	0.10000
2	Landsat 8 TIRS	11	$3.3420.10^{-4}$	0.10000

3.2. Conversion of the spectral radiance to brightness temperature

The Landsat thermal band data can be converted form spectral radiance to brightness temperature using following equation [14]:

$$T = \frac{K_2}{\ln\left(\frac{K_1}{L_\lambda} + 1\right)} \quad (3)$$

Where

T – At satellite brightness temperature (K)

K_1 – Calibration constant 1 [W/(m².sr.µm)]

K_2 – Calibration constant 2 [K]

Table 4. Landsat TM, ETM+ and Landsat 8 thermal band calibration constants [14]

No.	Data type	Band	K_1 (W/(m².sr.µm))	K_2 (Kelvin)
1	Landsat 5 TM	6	607.76	1260.56
2	Landsat 7 ETM+	6	666.09	1282.71
3	Landsat 8	10	774.89	1321.08
		11	480.89	1201.14

3.3. Estimation of surface emissivity

In this paper, the surface emissivity is determined by using method based on NDVI image, which proposed by Valor and Caselles (1996). For Landsat thermal band, the surface emissivity can be calculated by following equation [12]:

$$\varepsilon = \varepsilon_v.P_v + \varepsilon_s.(1 - P_v) \quad (4)$$

Where

ε – Surface emissivity

ε_v – Emissivity of pure vegetation covers area

ε_s - Emissivity of pure soil area

P_v - The percentage of vegetation in one pixel, which calculated by equation:

$$P_v = \left(\frac{NDVI - NDVI_{min}}{NDVI_{max} - NDVI_{min}}\right)^2 \quad (5)$$

NDVI – normalized difference vegetation index, which can be calculated by equation:

$$NDVI = \frac{NIR - RED}{NIR + RED} \quad (6)$$

Where RED and NIR – the spectral reflectance in red and near – infrared band, respectively.

3.4. Calculation of land surface temperature

In the final step, land surface temperature (LST) is estimated by the following equation:

$$LST = \frac{T}{1 + \frac{\lambda . T_B}{\rho} . ln\varepsilon} \quad (7)$$

Where

λ - The wavelength of the emitted radiance; T – brightness temperature; ρ – constant (1,438.10^{-2} m.K), which calculated by equation: $\rho = \frac{h.c}{\sigma}$, σ – Stefan Boltzmann's constant, which is equal to 5,67.10^{-8} ($Wm^{-2}.K^{-4}$); h – Plank's constant (6,626.10^{-34}J.sec); c – velocity of light (2.998.10^{8} m/sec).

4. Results and discussion

For determining surface emissivity by this methodology, values of soil and vegetation emissivity are needed. This study has been used more than 100 training samples for bare soil and vegetation cover areas to calculate normalized difference vegetation index (NDVI). Finally, NDVI for pure soil and pure vegetation cover of study area equal 0.125 and 0.510, respectively. Emissivity of pure soil and pure vegetation cover areas are calculated using method of Van de Griend (1993) by following equation [13]:

$$\varepsilon = 1.0094 + 0.047 \ln(NDVI) \quad (8)$$

Emissivity of pure soil and pure vegetation cover areas identified by using this method equal 0.912 and 0.978 respectively. On the basis of land surface temperature image, there was a good contrast between suspected coal fire area and surroundings. As seen on these images, subsurface coal fires in Khanh Hoa coal mine (northern) is clearly visible. Surface temperature in Khanh Hoa coal mine so much higher than in surroundings, even compare in urban area, which is characterized by impervious surfaces. The land surface temperature distribution map of the study area displays the different zone of temperatures. The density sliced image shows nine temperature zones that represents greater than 35, 33 – 35, 31 – 33, 29 – 31, 27 – 29, 25 – 27, 23 – 25, 21 – 23 and less than 21 ^{o}C respectively, in which areas of prominent temperature anomalies colored in red (Fig. 3 – 5).

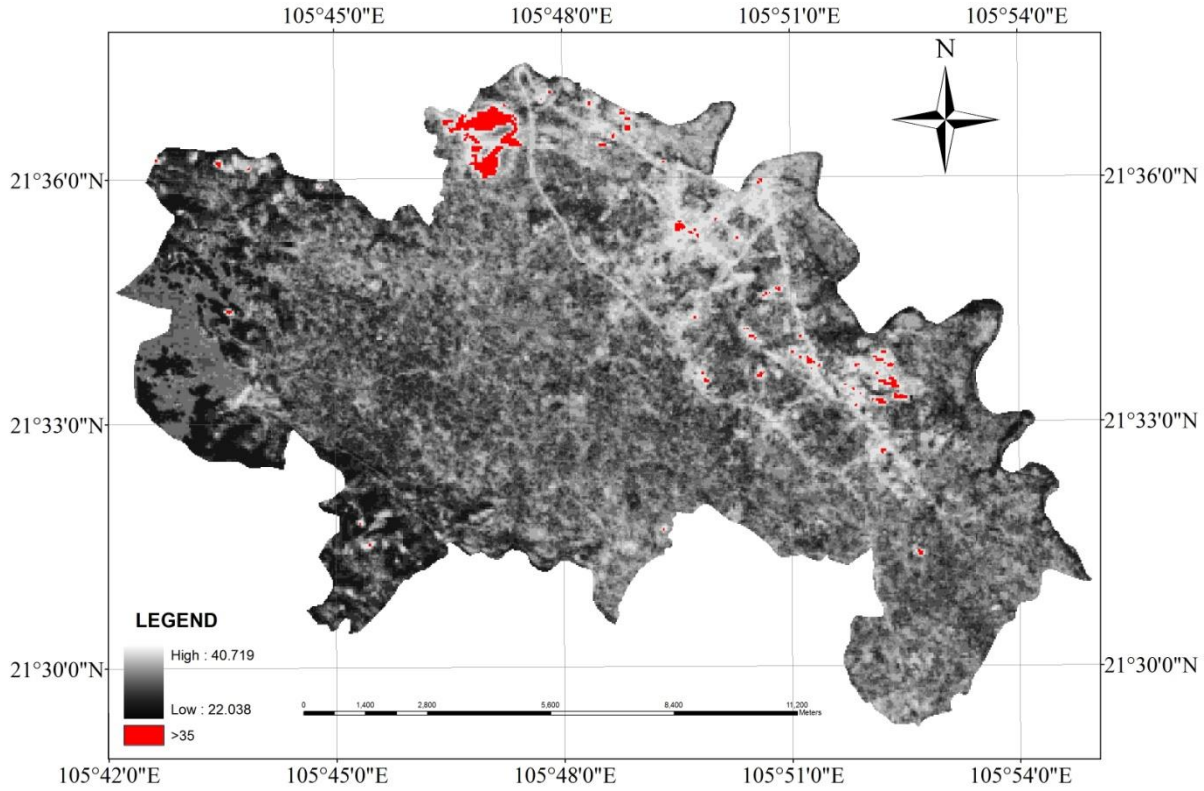

Figure 3. Subsurface coal fire in Khanh Hoa coal mine in 08 November 2007

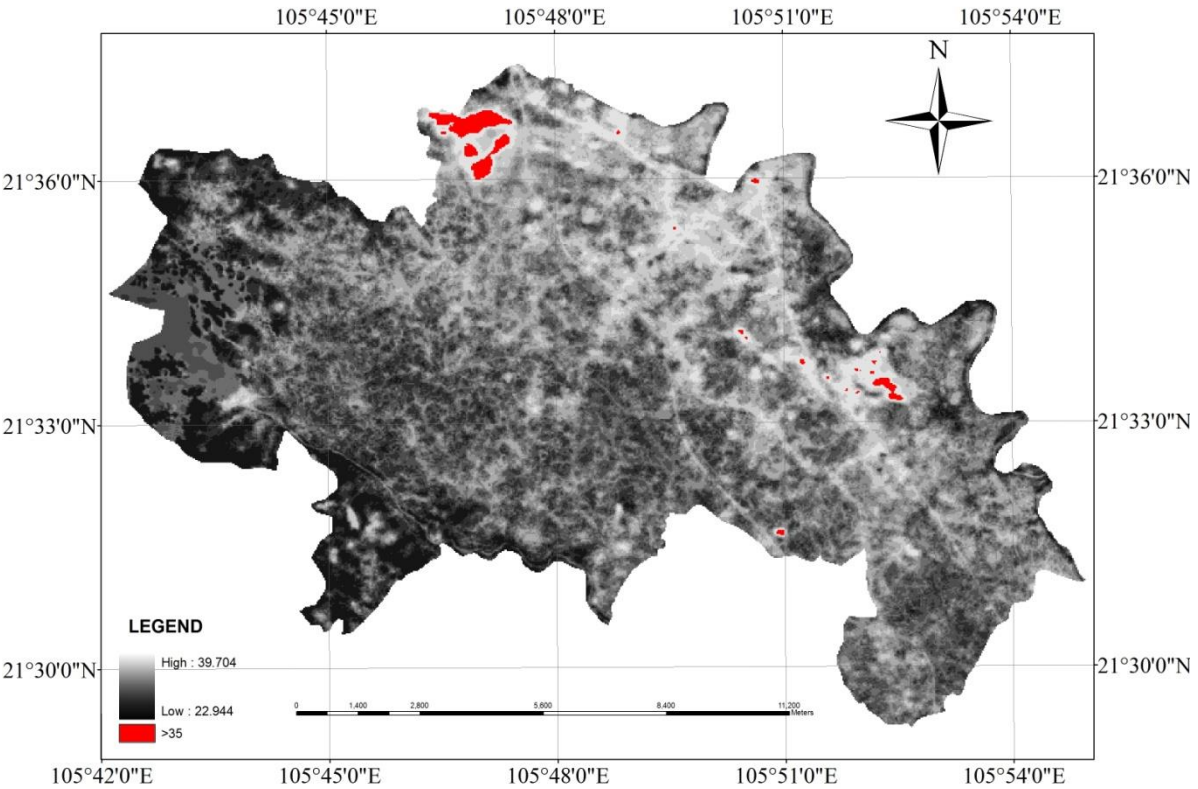

Figure 4. Subsurface coal fire in Khanh Hoa coal mine in 08 November 2010

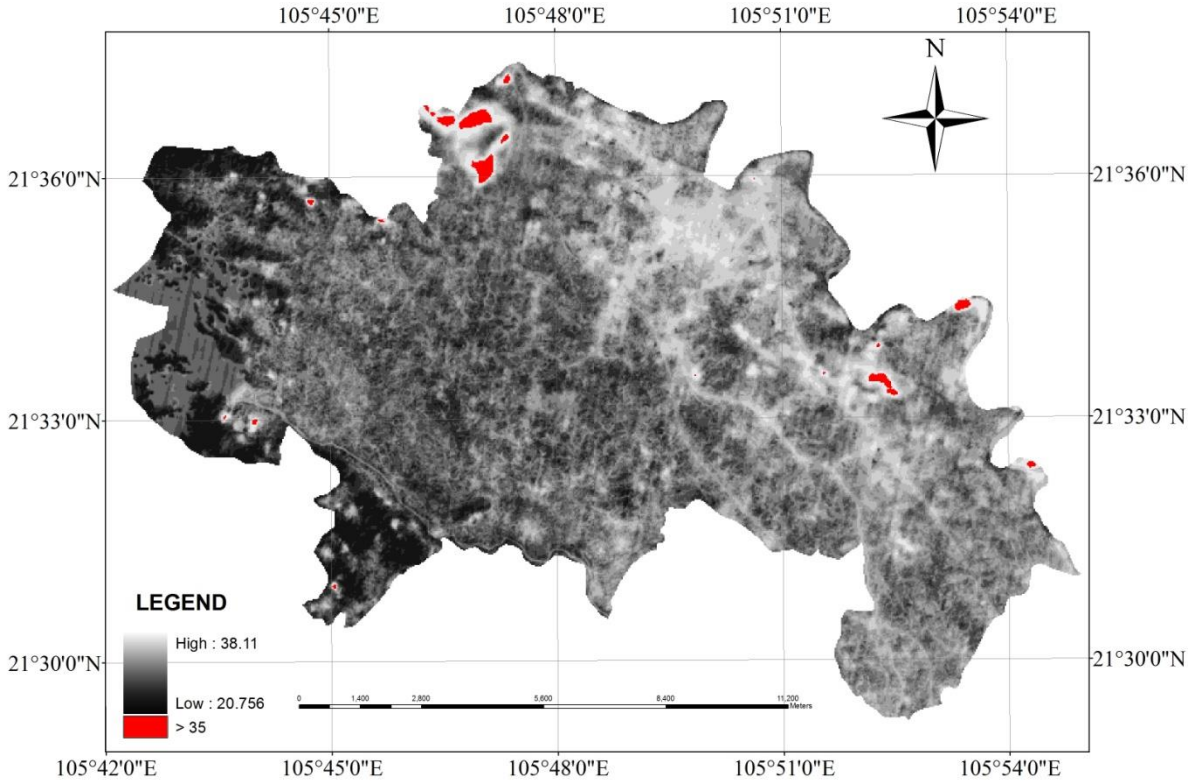

Figure 5. Subsurface coal mine in Khanh Hoa coal mine in 19 January 2014

The study shows that the total coal fire affected area was increased from 2007 to 2010 and reduced to 2014. The coal fire area in Khanh Hoa coal mine was found in increasing order 139.56 ha in 2007 to 158.76 ha in 2010 and decreasing to 74.43 ha in 2014 (Table 5). The fire area accounts for increase of 13.76 % during 2007 – 2010 and decrease of 53.12 % during 2010 – 2014.

Table 5. Subsurface coal fire area in different year calculated by Landsat data

No.	Time of data acquisition	Area of surface coal fires (ha)
1	8 November 2007	139.56
2	8 November 2010	158.76
3	19 January 2014	74.43

5. Conclusion

Coal fire is a dangerous phenomenon which affects seriously on the environment. Land surface temperature is higher in the zones of subsurface coal fire than in their surroundings areas. Remote sensing technique with many advantages compare tradition method has been used as a reliable tool for coal fire detecting and monitoring since 1960. In this study, multi-temporal Landsat TM, ETM+ and Landsat 8 thermal band data from 2007 to 2014 were used to calculate spectral radiance and converted to the brightness temperature. To retrieve the land surface temperature, the surface emissivity was estimated using NDVI index based on method developed by Valor and Caselles (1996) [12] and Van de Grined (1993) [13].

The dynamics of coal fires in Khanh Hoa coal mine during period of 2007 – 2014 were studied and calculated from the multi-temporal coal fire map. The subsurface coal fires areas increased from 139.56 ha in 2007 to 158.76 ha in 2010, and decreased to 74.43 ha in 2014. The results which are obtained in this study can be used to supervise of fire zones, giving warnings and measures to prevent this problem.

References

1. Luu Duc Hai, Nguyen Thi Hoang Lien (2009). *Renewable energy policies for sustainable development in Vietnam*, VNU Journal of Sciences, Earth Sciences, Vol. 25, Issue 3, 133 – 142.
2. Prakash, A., Gupta, R. P. (1999). *Surface fires in Jharia Coalfield, India - their distribution and estimation of area and temperature from TM data*, International Journal of Remote Sensing, 20, pp. 1935-1946.
3. Chen Y., Li J., Yang B., Zhang S. (2007). *Detection of coal fire location and change based on multi – temporal thermal remotele sensed data and field measurements*, International Journal of Remote Sensing, Vol. 28, Issue 15, pp. 3173 – 3179.
4. Cracknell A.P., Mansor S.B. (1992). *Detection of sub – surface coal fires using LANDSAT thematic mapper data*, International Archives of Photogrammetry and Remote Sensing, Vol. 29, pp. 750 – 753.
5. Prasun K., Kuntala L., Kanika S. (2005). *Application of remote sensing to dentify coal fires in the Raniganj coalbelt, India*, Internatinoal journal of Applied earth observation and Geoinformation, 117, 8 pp.
6. Mishra R.K., Roy P.N.S., Pandey J., Khalkho A., Singh V.K. (2014). *Study of coal fire dynamics of Jharia coalfield using satellite data*, International journal of Geomatics and Geosciences, Vol. 4, No. 3, 477 – 484.
7. Mishra R.K., Pandey J., Chaudhary S.K., Khalkho A., Singh V.K. (2012). *Estimation of air pollution concentration over Jharia coalfield based on satellite imagery of atmospheric aerosol*, International journal of Geomatics and Geosciences, Vol. 2, No. 3, 723 – 729.
8. Hongyuan Huo, Xiaoguang Jiang, Xianfeng Song, Zhao-Liang Li, Zhouya Ni, Caixia Gao (2014). *Detection of coal fire dynamics and propagation direction from multi-temporal nighttime Landsat SWIR and TIR data: A case study on the Rujigou coalfield, Northwest China*, Remote sensing, 6, 1234 – 1259.
9. Gautam R.S., Singh D., Mittal A. (2008). *An efficient contextual algorithm to detect subsurface fires with NOAA/AVHRR data*, IEEE Geoscience and Remote sensing, Vol. 46, Issue 7, 2005 – 2015.
10. Zhang J., Wagner W., Prakash A., Mehl H., Voidt S. (2004). *Detecting coal fires using remote sensing techniques*, International journal of Remote sensing, 25, 3193 – 3220.
11. Voigt S., Tetzlaff A., Zhang J., Kunzer C., Zhukov B., Strunz G., Oertel D., Roth A., Dijk P. van, Mehl H. (2004). *Integrating satellite remote sensing techniques for detection and analtsis of uncontrolled coal seam fire in North China*, International journal of coal geology, 59, 121 – 136.
12. Valor E., Caselles V. (1996). *Mapping land surface emissivity from NDVI. Application to European African and South American areas*, Remote sensing of Environment, 57, pp. 167–184.
13. Van de Griend A.A., Owen M. (1993). *On the relationship between thermal emissivity and the normalized difference vegetation index for natural surface*, International journal of remote sensing, 14, pp. 1119 – 1131.
14. National Aeronautics and Space Administration (NASA), *LANDSAT Science data user's Handbook*, 186 pp, http://landsathandbook.gsfc.nasa.gov/.
15. http://www.vinacomin.vn

УДК 63.54

Дистанционные методы мониторинга подземного угольного пожара: на примере угольной шахте Ханьхоа, провинция Тхайнгуен, Вьетнам

Ле Хунг Чинь

Технический университет им. Ле Куи Дон, Ханой, Вьетнам

Аннотация. Угольная шахта Хань Хоа, находящаяся в провинции ТхайНгуен, одно из крупнейших месторождений угля во Вьетнаме, где уголь добывается открытым способом.

По разным причинам, среди которых использование ненадлежащих технологий и несанкционированное недропользование, в этой местности происходят поверхностные и подземные угольные пожары. Подземные угольные пожары – опасные явления, сопровождаются выбросом ядовитых газов и лесным пожарами, пагубно влияют на весь регион. Данная работа посвящена применению серии разновременных тепловых ИК изображений LANDSAT для выявления подземных угольных пожаров. Полученные результаты могут эффективно использоваться при мониторинге подземных угольных пожаров и выработки предупреждающих мероприятий.

Ключевые слова: подземный угольный пожар, дистанционное зондирование, инфракрасная съемка, LANDSAT, поверхностная термодинамическая температура.